

# Mechanical Properties Of Acrylo Butadiene Styrene (Abs) Based Cellar Lattice Structures With Multi-Configuration

**Ramaprasad.H<sup>1</sup>, Shrinivasa Mayya D.<sup>1</sup>, N. R. Banapurmath<sup>2</sup>,  
Karthek Ravulapati<sup>3</sup>, M.A. Umarfarooq<sup>2</sup>**

<sup>1</sup>*Department of Mechanical Engineering, Srinivas University, Mukka, Mangalore – 574146, India,*

<sup>1</sup>*Department of Mechanical Engineering, Srinivas University, Mukka, Mangalore – 574146, India,*

<sup>2</sup>*Centre for Material Science, Department of Mechanical Engineering, KLE Technological University, Hubballi 580031, Karnataka, India*

<sup>3</sup>*Collins Aerospace, 5935, Pinnacle View Road, Cumming GA 30040, United States*

<sup>2</sup>*Centre for Material Science, Department of Mechanical Engineering, KLE Technological University, Hubballi 580031, Karnataka, India*

*Corresponding author: Ramaprasad.H*

*([ramptech2002@gmail.com](mailto:ramptech2002@gmail.com), [principalsit@srinivasgroup.com](mailto:principalsit@srinivasgroup.com),  
[nr\\_banapurmath@kletech.ac.in](mailto:nr_banapurmath@kletech.ac.in), [kartheek.ravulapati@gmail.com](mailto:kartheek.ravulapati@gmail.com),  
[umarfarooq.ma@gmail.com](mailto:umarfarooq.ma@gmail.com))*

Cellular lattice structures (CLS) are pivotal in manufacturing sectors due to their high-strength, light weight and customization potential making them ideal for advanced applications. Acrylo Butadiene Styrene (ABS) based CLS samples are prepared by fused deposition modeling (FDM) additive manufacturing method by combining multi-configuration arrangements. In the first phase of the work, 3D printed ABS based CLS structures with triangular, square, and hexagonal cellular shapes are printed with horizontal and vertical cell orientations. In the second phase of the work, 3D printed CLS structures with cubic lattice and truss structures viz fluorite, FCC, BCC lattice and ISO truss are printed. Specimens are tested by the universal testing machine to determine bending stress, equivalent bending stiffness, compressive stress, and Shore hardness of CLS samples. Hexagonal cell structures exhibited higher bending strength compared to triangular and square cell structures with cells oriented in horizontal and vertical direction. Further vertically oriented hexagonal CLS exhibited a higher bending strength of 1200 N compared to its horizontal cell orientation of 800 N. ISO truss and Fluorite cubic lattices exhibited a higher bending-dominated deformation with bending strength of 350 N, 325 N followed by FCC and BCC lattices. Among the different lattice structures tested hexagonal cellular lattice structure with vertical orientation exhibited maximum bending stiffness of  $2.03 \times 10^4$

N/m<sup>2</sup> compared to  $0.98 \times 10^4$  N/m<sup>2</sup> with horizontal cell orientation. Hexagonal cell structures exhibited higher compressive strength compared to triangular and square cell structures with cells oriented in both horizontal and vertical direction. Further vertically oriented hexagonal CLS exhibited a higher compressive strength of 3000 MPa compared to its horizontal cell orientation of 2620 MPa. Fluorite consistently exhibited the highest compressive strength and strength-to-weight ratio compared to BCC and FCC structures followed by ISO truss. Vertical cell orientation of all the cellular lattice structures exhibited higher shore hardness compared to their counterparts with cells oriented in horizontal direction. Further vertically oriented hexagonal CLS exhibited a higher Shore hardness of 66 compared to its horizontal cell orientation of 61 MPa. Truss structures (ISO) exhibited higher Shore hardness values (33) followed by BCC cubic and fluorite lattice.

**Keywords:** Cellular lattice structures, Acrylo Butadiene Styrene, hexagonal, bending strength, compressive stress, and Shore hardness.

## 1. Introduction

Advanced rapid prototyping and rapid manufacturing greatly assist in creating physical models and functional prototypes sourced directly from CAD models. Further additive manufacturing focusses on layer-based automated rapid prototype manufacture process to generate 3-dimensional objects directly from CAD data without part-depending tools. Additive manufacturing (ADM) is slowly progressing from prototyping applications to manufacturing of functional products. ADM has four categories based on the materials they use: polymer, metallic, ceramic, biological and functional materials. Complex designs, and designs that once were considered impossible or impractical, can be realized with ADM [1]. Advancements in AMD, has facilitated creating complex geometries with cellular geometries using different materials. Recently advances in additive manufacturing has promoted swift development of these lattice structures. Salient features of cellular materials include lightweight, higher specific stiffness, higher specific strength and improved designability provide lightweight designs. Further increased porosity, lower relative density, periodic arrangement with enhanced heat dissipation and energy absorption are additional characteristics of cellular lattice structures [2, 3, 4, 5]. Cellular lattice structures greatly reduce the weight of the parts [6,7] and find applications in aerospace, machinery, medical field, construction field [8,9]. Uniform lattice shapes can be quickly shaped by periodic arrangement of cells and based on topological cells configurations they can be grouped into grid structure [10], honeycomb structure [11], truss structure [12], sandwich structure [13] and cubic lattice structure [14,15]. Nucleation and spread of cracks in triangular, square, hexagonal, kagome-type cells based cellular materials were reported in the literature [16–19]. Stress formed by parts under external load frequently presents inhomogeneous distribution characteristics of these materials when used in real time applications. Mechanical properties of these materials, can be improved with variable density lattice structure. It is reported that stiffness of lattice structures can be pointedly improved by appropriately adjusting material distribution using compression tests and finite element analysis [20]. Compared with uniform lattice structure, variable density lattice structure and multi-configuration lattice structures have exhibited improved mechanical properties.

From the exhaustive literature survey carried out on less research is reported on bio-inspired CLS structures for structural applications. The objectives of present work is to evaluate the mechanical properties of the different ABS based 3D printed cellular lattice structures. Multi-configuration design for improved composite lattice arrangement mode, and the relevant parameter for evaluating mechanical properties are explored. The novelty of the work involves synthesis of 3D printed ABS CLS with different multi-configuration. Future scope of the work involves study on 3D printed ABS CLS nano-composites dispersed with carbon derived nanoparticles such as carbon nanotubes, graphene, graphene amine etc.

2.0. Samples and experiment

2.1. Arrangement of cellular lattice structures with multi-configuration

CLS structures derived from ABS with triangular, square, and hexagonal cell shapes oriented in both horizontal and vertical directions are 3D printed. In addition, cubic lattice, and truss structures viz fluorite, FCC, BCC lattice and ISO truss are 3D printed. Limitation of the process and printing accuracy, cell size can only be taken within the manufacturable range.

2.5.1. Lattice structure samples

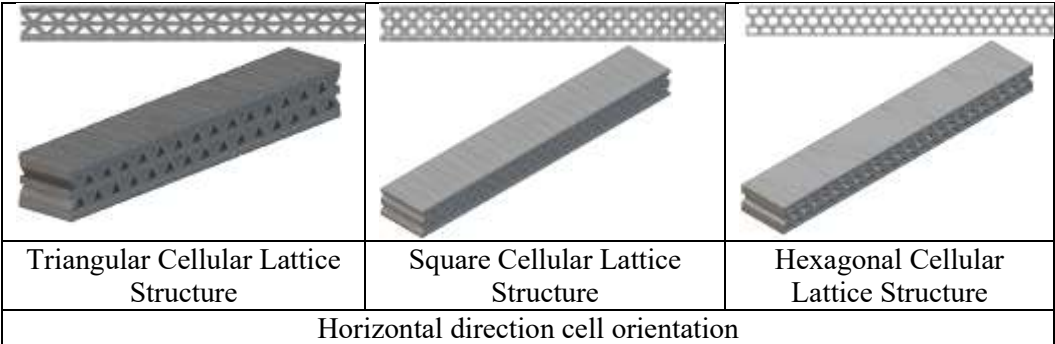
A Fractal 3D printer used has a molding range of 300 mm × 300 mm, with printing layer thickness being 0.15 mm ~ 0.45 mm, and the forming accuracy is 0.05 mm.

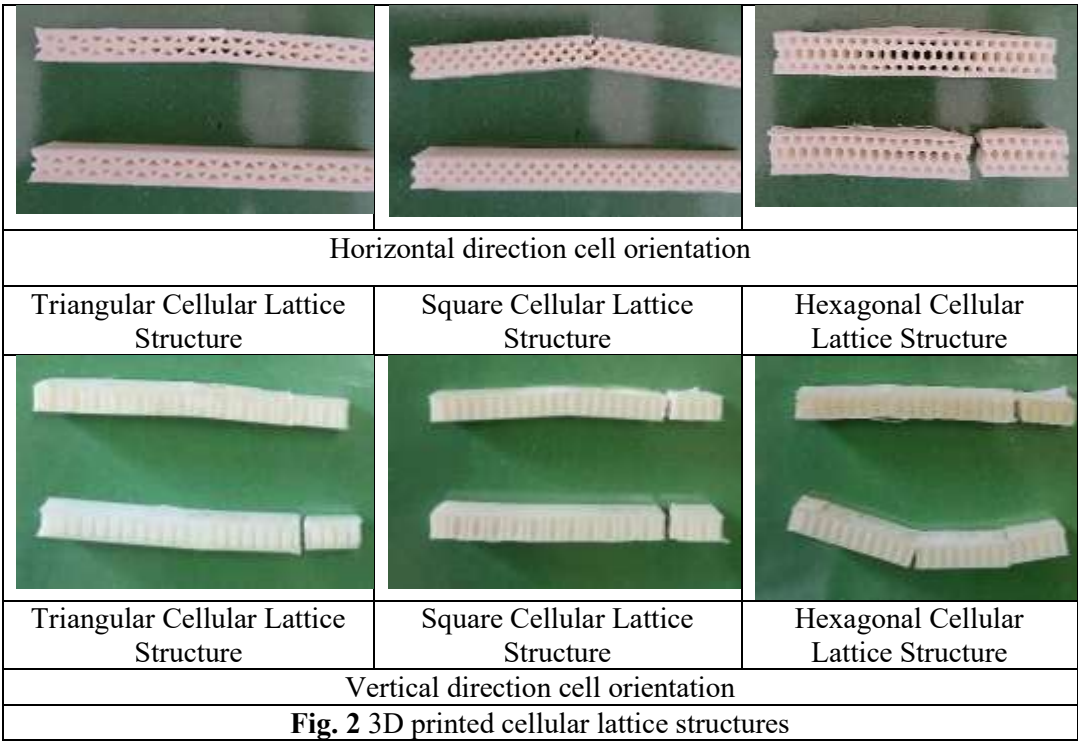
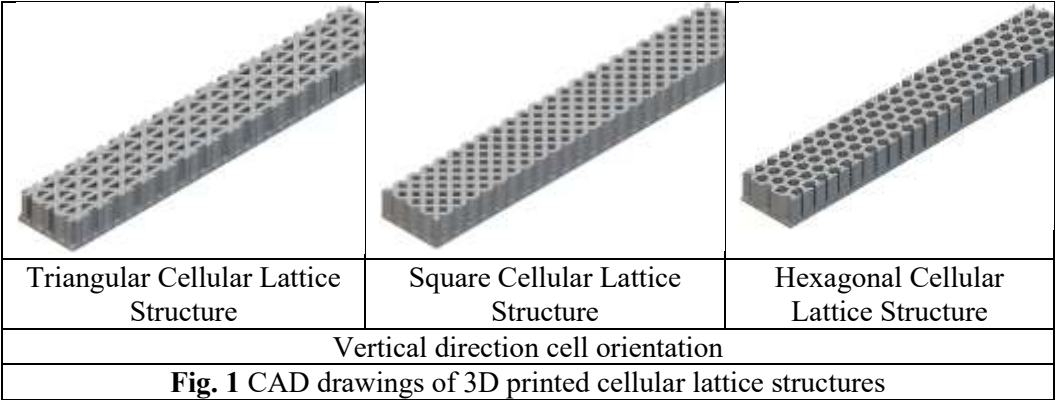
Factory Software – printing and slicing details:

Make: Julia 250 Dual, Nozzle: Model 0.6 mm, Layer height 0.15 – 0.45, Speed: 50 mm/s, Printing Temp 210°C, build plate temp 60°C.

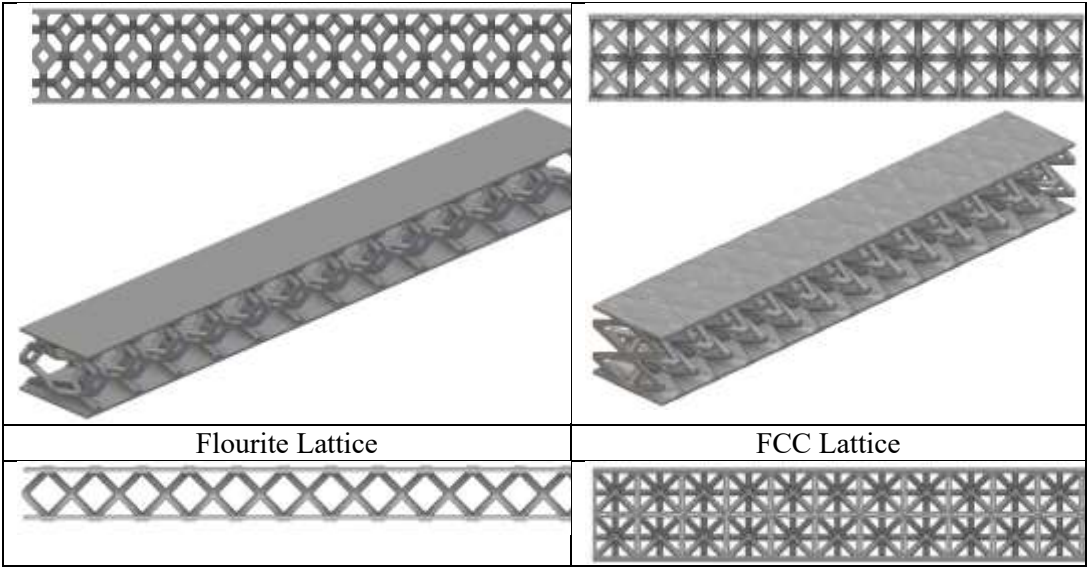
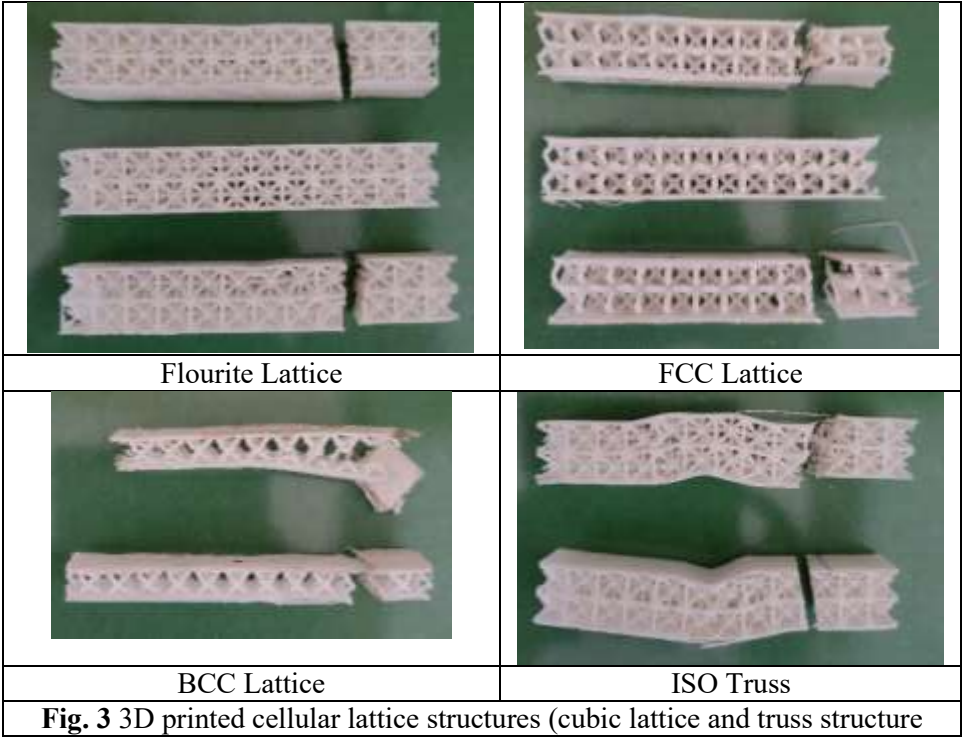
The ABS is used for lattice structure sample preparation and the properties of ABS are density  $\rho= 0.95 \text{ g/cm}^3$ , elastic modulus  $E = 1.8 \text{ GPa}$ , Poisson’s ratio  $\nu = 0.3$ , printing temperature: 220-260°C.

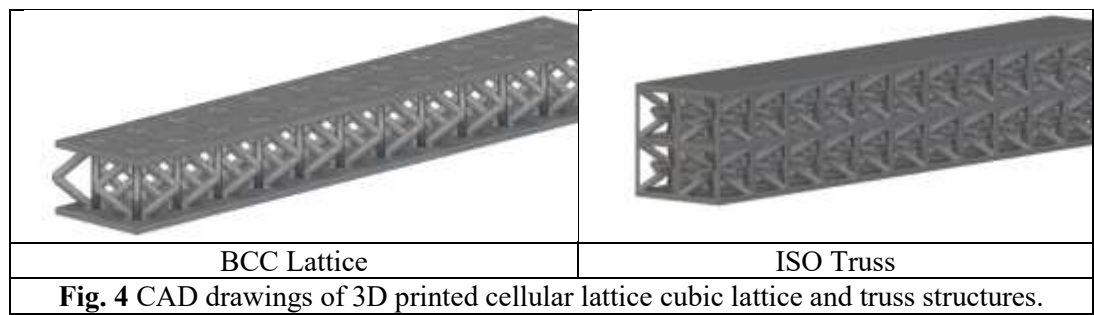
In the first phase of the work, 3D printed CLS structures with triangular, square and hexagonal cellular shapes are printed with different cell orientations. Figure 1 shows the CAD drawings of the CLS with horizontal and vertical cell orientation. Figure 2 shows these 3D printed CLS.





In the second phase of the work, 3D printed CLS structures with cubic lattice and truss structures viz fluorite, FCC, BCC lattice and ISO truss are printed. Figure 3 shows the CAD drawings of cubic lattice and truss structures. Figure 4 shows these 3D printed cubic lattice and truss CLS.





3.0 Results and discussion

The 3D printed CLS samples are subjected to mechanical testing to determine load-deformation, bending stiffness, compressive stress and hardness and compare the properties [21, 22].

Triangular and square cells based 3D-printed ABS cellular structures exhibit higher tensile strength and strength-to-weight ratios when compared to hexagonal structures because of higher energy absorption capacity. Hexagonal cell structures known for their efficient space packing, strong weight distribution and structural integrity, exhibit lower tensile strength compared to square or triangular cells.

3.1 Bending stress of CLS samples

3.1.1 Load-deformation behavior of 3D printed CLS with different cell shape and orientation

Figures 5 and 6 shows load-deformation curves for ABS based CLS with horizontal and vertical cell orientation. The shape of the individual cells viz hexagonal, triangular, square CLS can impact the overall strength and deformation behavior of the material.

From the figures 5 and 6 it follows that hexagonal cell structures exhibited higher bending strength compared to triangular and square cell structures. This is mainly attributed to hexagonal configuration that supports a more uniform stress distribution, higher energy absorption and better transfer of external forces leading to increased tensile and impact strength. Hence this configuration finds many engineering applications where bending and impact resistance is essential.

Effect of cell orientation on bending strength of the CLS:

Bending strength of the CLS structures is greatly affected by the cell orientation. All the vertically oriented hexagonal, triangular, square cell structure exhibited higher bending strength than a horizontally oriented one. This is because the geometry of the cell structures in the vertical orientation allows for greater resistance to bending moments, whereas the horizontal orientation may lead to more pronounced buckling or deformation under bending loads. When cell structure are oriented vertically, the cell walls primarily resist bending loads by supporting the weight or forces applied to the structure. This arrangement allows for a more



stable and rigid structure, enhancing its bending strength. In contrast, when the cell structure is oriented horizontally, the cell walls are subjected to bending loads that can lead to more pronounced buckling or deformation. This can result in reduced bending strength compared to the vertical orientation. Regardless of orientation, hexagonal cell structure exhibited higher bending strength followed by triangular and square structures considered in the study. Figure 7 and shows the effect of cell orientation on bending stiffness of hexagonal cellular lattice structures.

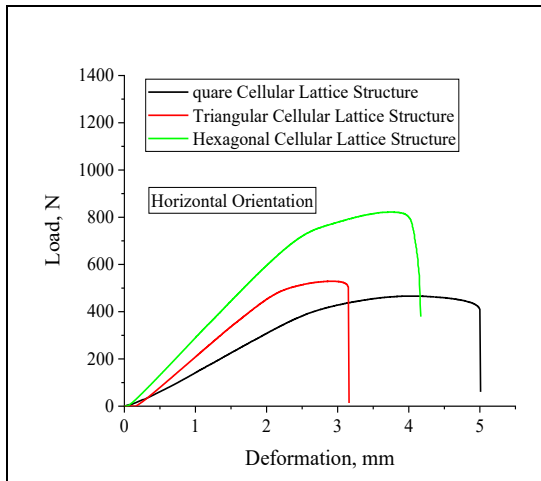


**Fig. 5** Load-deformation curves for CLS with horizontal cell orientation

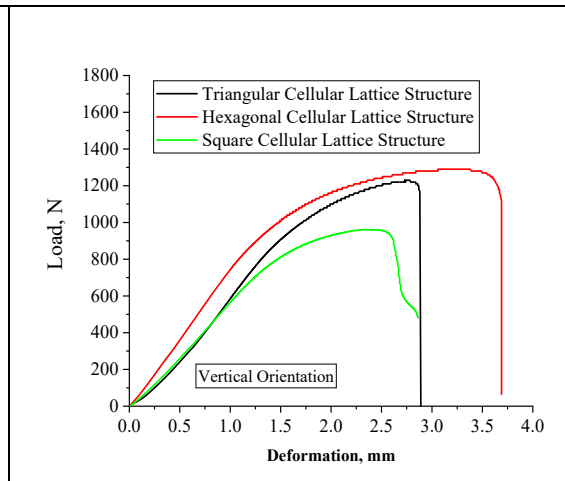


**Fig. 6** Load-deformation curves for CLS with vertical cell orientation

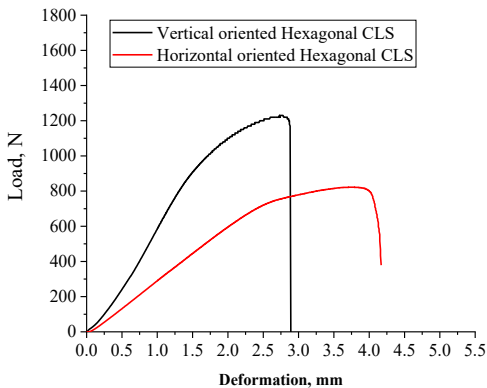


**Fig. 7** Effect of cell orientation on bending strength of hexagonal CLS

### 3.1.2 Load-deformation behavior of 3D printed cubic lattice and truss structures

Load-deformation behaviour of cubic lattice and truss structures are shown in Fig. 8. Bending stiffness signifies ability of the material to resist bending deformation. The equivalent bending stiffness coefficient provides bending resistance of lattice structure. From figure 8 it is found that ISO truss tend to have better deformation resistance and can offer superior bending stiffness and ductility compared to cubic lattices which often show less favorable bending performance.

3D-printed BCC, FCC, and fluorite cubic lattice structures exhibit distinct bending stress behaviors. Fluorite cubic lattices exhibited a bending-dominated deformation behavior compared followed by FCC and BCC lattice as shown in fig. 8. FCC lattices, with their higher connectivity are more resistant to bending compared to BCC. BCC lattices due to their lower connectivity tend to bend under stress rather than stretch or compress compared to FCC as shown in fig. 8.

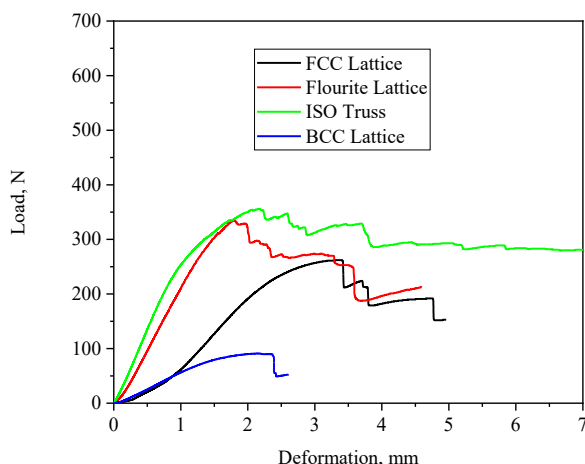


**Fig. 8** Load-deformation curves for cubic lattice and truss structures

### 3.1.3 Equivalent bending stiffness (k)

Lattice structure can be taken to be comparable to a uniform solid material with a certain density, stiffness, and strength with reference to equivalent material method [21, 23, 24, 25]. Formula of solid materials can be used for with equivalent analysis of mechanical properties of lattice structure materials approximately.

Deflection formula of simply supported beam is as follows:

$$w_{\max} = \frac{Fl^3}{48EI} = \frac{Ml^2}{12EI} \quad \text{---(1)}$$

Equivalent bending stiffness of the lattice structure is given as below:

$$k_w = EI = \frac{Fl^3}{48w_{\max}} \quad \text{---(2)}$$

Equivalent bending stiffness of the different samples is calculated using equation (2) as shown in table 1. From the table 1 it follows that Cellular Lattice Structure with horizontal and vertical



cell orientation exhibited higher equivalent bending stiffness compared to cubic lattice and truss structures. Among the different lattice structures tested hexagonal cellular lattice structure with vertical orientation exhibited maximum bending stiffness.

**Table 1** Equivalent bending stiffness of CLS

Sl. No.	Cellular Lattice Structure	Equivalent bending stiffness (k) in ( $\times 10^4$ ) N/m <sup>2</sup>
<b>Cellular Lattice Structure with horizontal orientation</b>		
1.	Hexagonal Cellular Lattice Structure	0.98
2.	Triangular Cellular Lattice Structure	0.84
3.	Square Cellular Lattice Structure	0.54
<b>Cellular Lattice Structure with vertical orientation</b>		
4.	Hexagonal Cellular Lattice Structure	2.03
5.	Triangular Cellular Lattice Structure	1.86
6.	Square Cellular Lattice Structure	1.75
<b>Cubic lattice and truss structures</b>		
7.	BCC composite lattice	0.19
8.	FCC lattice	0.36
9.	Fluorite lattice	0.73
10.	ISO Truss lattice	0.84

**3.2 Compressive stress of Cellular lattice structures:**

**3.2.1 Compressive stress of 3D printed CLS with different cell shape and orientation**

Figures 9 and 10 shows the compressive stress for ABS based CLS with horizontal and vertical cell orientation. The shape of the individual cells viz hexagonal, triangular, square CLS can impact the overall compressive stress behavior of the material. Hexagonal, triangular, and square lattice structures exhibit different compressive strengths. Hexagonal lattice structures exhibit higher compressive strength followed by triangular and square structures, while square structures may offer a balance between strength and weight.

Hexagonal lattice structures often referred to as honeycomb structures exhibit higher compressive strength and energy absorption due to their efficient material usage and buckling resistance as shown in figure 9. Their ability to resist buckling under compressive loads makes them suitable for applications requiring high strength and stiffness. Triangular structures offer a good balance between strength and weight, and their geometry can be adapted for specific load-bearing requirements. Square structures offer a straightforward approach to lattice design and can be easily fabricated. Their compressive strength is generally lower than hexagonal and triangular structures as shown in figure 9.

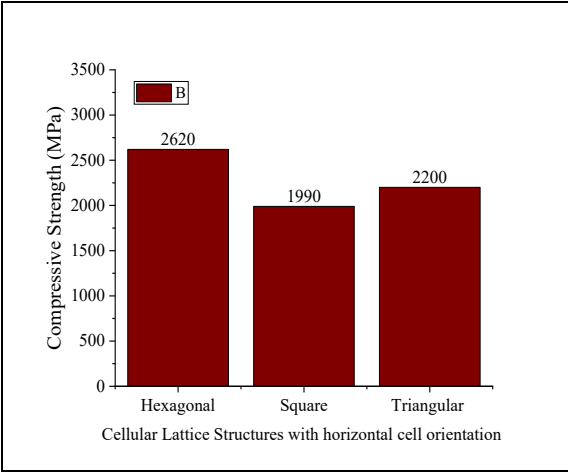


**Fig. 9** Compressive strength for CLS with horizontal cell orientation

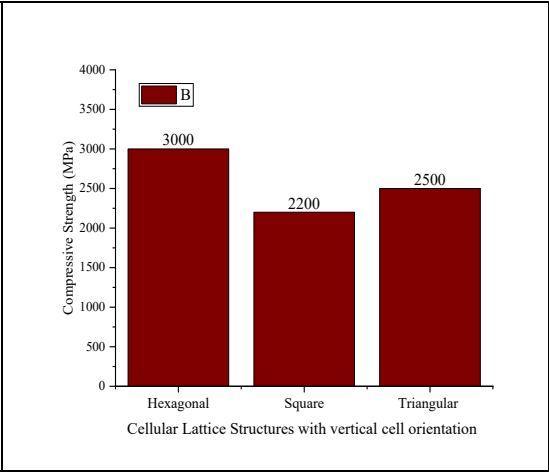


**Fig. 10** Compressive strength for CLS with vertical cell orientation

**Effect of cell orientation on compressive strength of the CLS:**

The compressive strength of 3D-printed hexagonal, triangular, and square cubic lattice structures varies depending on cell orientation (vertical or horizontal) and the specific lattice type. Hexagonal, triangular, and square cubic lattice structures with vertical cell orientation tend to possess higher compressive strength compared to those with horizontal cell orientation exhibiting better energy absorption capabilities as shown in figure 11. This is because the vertical cells directly resist the applied compressive force. Structures with horizontal cells may be less strong in compression, especially if the compressive load is applied in the vertical direction. The horizontal cells may buckle or deform under the load, leading to lower compressive strength.

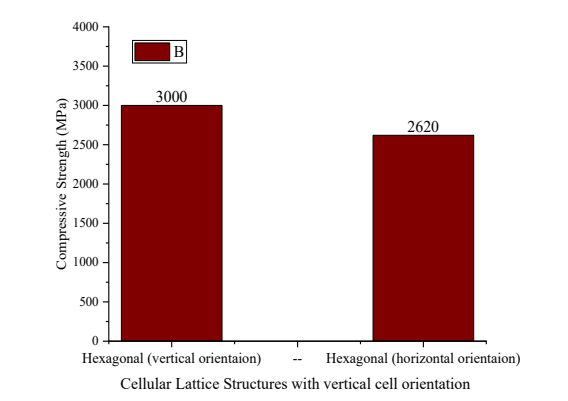


**Fig. 11** Effect of cell orientation on compressive strength of hexagonal CLS

### 3.2.2 Compressive stress of 3D printed cubic lattice and truss structures

Fig. 12 shows the compressive strength for cubic lattice and truss structures. In 3D printed lattice structures, fluorite consistently exhibits the highest compressive strength and strength-to-weight ratio compared to BCC and FCC structures followed by ISO truss. Fluorite lattices make them suitable for high-strength applications where minimal weight is critical.

BCC, while having the lowest strength-to-weight ratio, shows a prolonged period of strain, indicating greater toughness making them suitable where a high amount of energy absorption is desired. FCC offers a balance between strength and energy absorption capacity and exhibit stretching-dominated deformation under compressive loads, which is a key factor in determining their mechanical behavior.

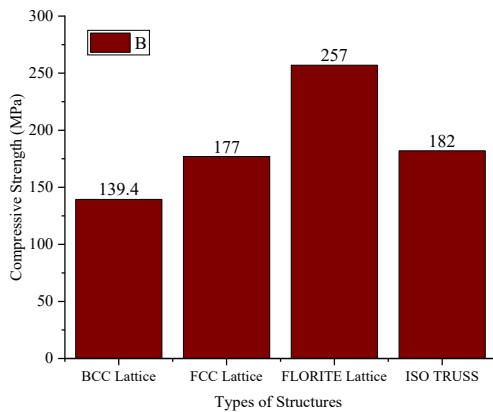
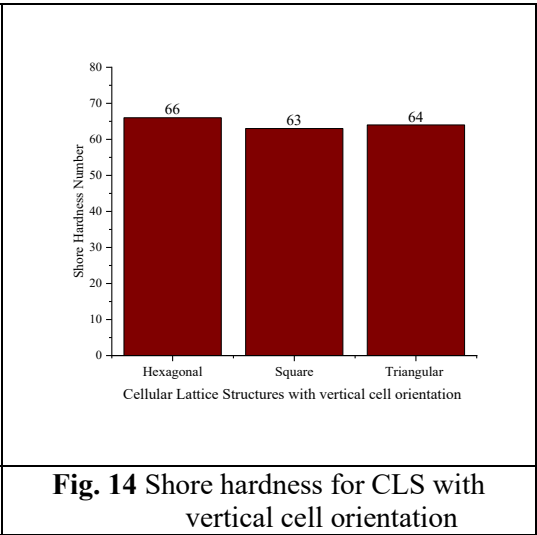
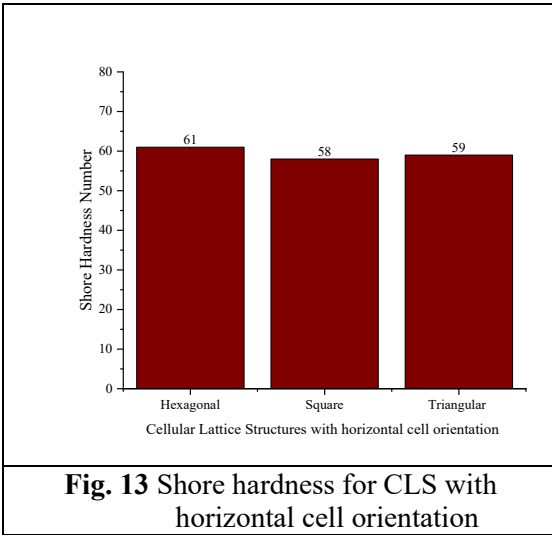


**Fig. 12** Compressive strength for cubic lattice and truss structures

### 3.3 Shore hardness of Cellular lattice structures:

#### 3.3.1 Shore hardness of 3D printed CLS with different cell shape and orientation

Generally, a higher Shore D hardness indicates a harder material. The Shore hardness of 3D printed cellular lattice structures can vary significantly depending on the material and lattice design (hexagonal, triangular, and square). Among these hexagonal CLS exhibited higher Shore hardness followed by triangular, and square structures.



**Effect of cell orientation on Shore hardness of the CLS:**

It can be seen from figures 14 and 15 that for vertical cell orientation of all the cellular lattice structures exhibited higher shore hardness compared to their counterparts with cells oriented in horizontal direction. The Shore hardness of 3D-printed hexagonal, triangular, and square cubic lattice structures varies depending on cell orientation (vertical or horizontal) and the specific lattice type. Hexagonal, triangular, and square cubic lattice structures with vertical cell orientation tend to have higher Shore hardness compared to those with horizontal cell orientation exhibiting better energy absorption capabilities. As shown in figure 11 hexagonal CLS with cell oriented in vertical direction exhibited higher shore hardness compared to horizontal one. This is because the vertical cells directly resist the applied force. Structures with horizontal cells may be less strong in hardness, especially if the load is applied in the vertical direction. The horizontal cells may buckle or deform under the load, leading to lower hardness.

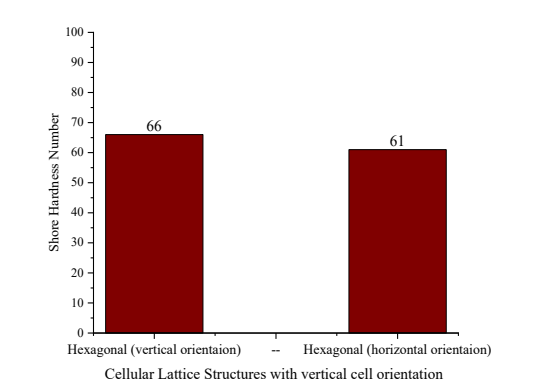


**Fig. 15** Effect of cell orientation on Shore hardness of hexagonal CLS

### 3.3.2 Shore hardness of 3D printed cubic lattice and truss structures

Shore hardness values for cubic lattice and truss structures can vary depending on specific structure design. Truss structures (ISO) are often designed to be more flexible than cubic lattices, and exhibited higher Shore hardness values followed by BCC cubic and fluorite lattice. BCC cubic lattices potentially showed higher hardness due to their higher density and more interconnectedness.

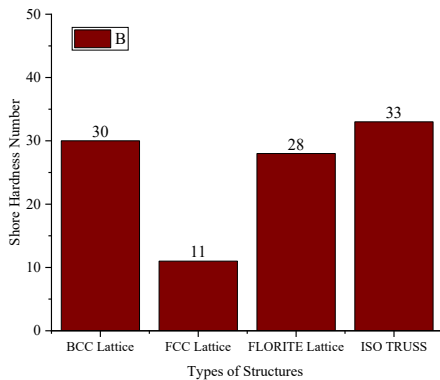


**Fig. 10** Shore hardness for cubic lattice and truss structures

### Conclusions

Experimental tests were conducted to determine bending stress, equivalent bending stiffness, compressive stress, and Shore hardness of 3D printed ABS based CLS structures. From the results the following conclusions were drawn:

- Among the different CLS samples hexagonal cell based structures exhibited higher bending strength compared to triangular and square cell structures with cells oriented in horizontal and vertical direction.
- Vertically oriented hexagonal CLS exhibited an increase of 50% higher bending strength compared to its horizontal cell orientation.
- ISO truss and Fluorite cubic lattices exhibited a higher bending-dominated deformation with bending strength of 350 N, 325 N followed by FCC and BCC lattices.
- Hexagonal cellular lattice structure with vertical orientation exhibited higher bending stiffness of 107% compared to its horizontal cell orientation.
- Hexagonal cell structures exhibited higher compressive strength compared to triangular and square cell structures with cells oriented in both horizontal and vertical direction.
- Vertically oriented hexagonal CLS samples exhibited a higher compressive strength of 14.52% compared to its horizontal cell orientation.
- Fluorite consistently exhibited the highest compressive strength and strength-to-weight ratio compared to BCC and FCC structures followed by ISO truss.

- Vertically oriented hexagonal CLS exhibited a higher Shore hardness of 8.19% compared to its horizontal cell orientation.
- Truss structures (ISO) exhibited higher Shore hardness values followed by BCC cubic and fluorite lattice.
- The 3D printed ABS based Hexagonal CLS samples with vertical cell orientation provides improved mechanical properties for bio-inspired structural engineering solutions.

## References

1. Hanser Publications, Cincinnati, Understanding Additive Manufacturing, Rapid Prototyping · Rapid Tooling, Rapid Manufacturing, Andreas Gebhardt Hanser Publishers, Munich Hanser Publications, ISBN 978-3-446-42552-1, Cincinnati.
2. Schaedler T.A., and Carter W.B., Architected Cellular Materials. Annual Review of Materials Research Volume 46, 2016, 46, 187–210.
3. Chougrani L, Pernot JP, V'eron P, et al. Lattice structure lightweight triangulation for additive manufacturing. *Comput-Aided Des* 2017; 90:95–104.
4. Zhong H, Gadipudi VK, Salem DR. Topology Optimization of Lightweight Lattice Structural Composites Inspired by Cuttlefish Bone. *Appl Compos Mater* 2018; 26(9): 1–13.
5. Gorguluarslan RM, Gandhi UN, et al. Design and fabrication of periodic lattice based cellular structures. *Comput Aided Des Appl* 2016; 13:50–62.
6. Fan HL, Jin FN, Fang DN. Mechanical properties of hierarchical cellular materials: Part I Analysis. *Compos Sci Technol* 2008;68(15–16):3380–7.
7. Chan YC, Shintani K, Chen W. Robust topology optimization of multi-material lattice structures under material and load uncertainties. *Front Mech Eng* 2019;14 (2):141–52.
8. Ying GA, Zz A, Hong HB, et al. New concept of carbon fiber reinforced composite 3D auxetic lattice structures based on stretching-dominated cells. *Mech Mater* 2020; 152:103661.
9. Plocher J, Panesar A. Review on design and structural optimization in additive manufacturing: Towards next-generation lightweight structures. *Material Design* 2019; 183:108164.
10. Kessler J, B'alc N, Gebhardt A, et al. Basic Research on Lattice Structures Focused on the Tensile Strength. *Applied Mech Mater* 2015; 808:193–8.
11. Shroff S, Acar E, Kassapoglou C. Design, analysis, fabrication, and testing of composite grid-stiffened panels for aircraft structures. *Thin-Walled Struct* 2017; 119:235–46.
12. Saigal A, Tumbleston J. Stress-Strain Behavior of an Octahedral and Octet-Truss Lattice Structure Fabricated Using the CLIP Technology. *Adv Mater Res* 2017;1142: 245–9.
13. Murtazaeva AK, Magomedov MA, Ramazanov MK. Phase Diagram and Structure of the Ground State of the Antiferromagnetic Ising Model on a Body-Centered Cubic Lattice. *JETP Lett* 2018; 107:259–63.
14. Vrana R, Koutny D, Palousek D. Impact resistance of different types of lattice structures manufactured by SLM. *MM Sci J* 2016;2016(6):1579–85.
15. Vaissier B, Pernot JP, Chougrani L, et al. Parametric design of graded truss lattice structures for enhanced thermal dissipation. *Computer-Aided Des* 2019; 115:1–12.
16. Lipperman F, Ryvkin M, Fuchs MB. Fracture toughness of two-dimensional cellular material with periodic microstructure. *Int J Fract* 2007;146:279–90.
17. Kueh ABH, Kho VT. Strut waviness and load orientation affected fracture toughness knockdown in biaxially woven square lattices. *Int J Mech Sci* 2019;164:105172.

18. Kueh ABH, Siaw YY. Impact resistance of bio-inspired sandwich beam with side arched and honeycomb dual-core. *Compos Struct* 2021; 275:114439.
19. Lipperman F, Ryvkin M, Fuchs MB. Nucleation of cracks in two-dimensional periodic cellular materials. *Comput Mech* 2007; 39:127–39.
20. Niknam H, Akbarzadeh AH. Graded lattice structures: Simultaneous enhancement in stiffness and energy absorption. *Mater Des* 2020; 196:109129.
21. Qing Z, Hualin F. Equivalent continuum method of plane-stress dominated plate lattice materials. *Thin-Walled Struct* 2021; 164:107865.
22. Lynch, Matthew E, Mordasky, et al. Design, testing, and mechanical behavior of additively manufactured casing with optimized lattice structure. *Additive Manufacturing* 2018; 22:462-471.
23. Niknam H, Akbarzadeh AH. Graded lattice structures: Simultaneous enhancement in stiffness and energy absorption. *Mater Des* 2020; 196:109129.
24. Namvar N, Zolfagharian A, Vakili-Tahami F, Bodaghi M. Reversible energy absorption of elastoplastic auxetic, hexagonal, and AuxHex structures fabricated by FDM 4D printing. *Smart Mater Struct* 2022;31(5):055021.
25. Ashok Dara MV, Raju Bahubalendruni A, Johnney Mertens A, Balamurali G. Numerical and experimental investigations of novel nature inspired open lattice cellular structures for enhanced stiffness and specific energy absorption. *Mater Today Commun* 2022; 31:2352–4928.